

X-ray photoelectron spectroscopy and theory of the valence band and semicore Ga 3d states in GaN

W. R. L. Lambrecht and B. Segall

Department of Physics, Case Western Reserve University, Cleveland, Ohio 44106-7079

S. Strite,* G. Martin, A. Agarwal, H. Morkoç, and A. Rockett

Materials Research Laboratory, University of Illinois at Urbana-Champaign, 105 South Goodwin Avenue, Urbana, Illinois 61801

(Received 23 June 1994)

The effects of the Ga 3d semicore levels on the electronic structure of GaN are discussed. While band-structure theory using the local-density approximation predicts these states to overlap with the N 2s band and to have important effects on the total energy, x-ray photoelectron spectroscopy (XPS) shows that they occur ~ 3 eV below the N 2s band. This apparent discrepancy is resolved by means of a so-called Δ SCF or difference of self-consistent-fields calculation, in which the binding energy is calculated as a total-energy difference including solid state screening effects by means of the excited-atom model. The calculated valence-band densities of states are found to be in good agreement with the XPS spectrum. The differences between zinc blende and wurtzite GaN are discussed.

I. INTRODUCTION

GaN and related group-III-nitrides (InN and AlN) being direct wide-band-gap semiconductors are of great interest for short-wavelength optoelectronics¹ as demonstrated by the recent development of efficient blue-violet light-emitting *pn* diodes by Akasaki *et al.*² A study of the electronic structure of these materials is important for many of the envisioned applications.

Although many band-structure investigations³⁻¹³ have appeared, a somewhat controversial issue is the nature of the Ga 3d semicore states. Most pseudopotential calculations⁸⁻¹¹ with the exception of the calculations by Wright and Nelson¹² and Neugebauer and Van de Walle¹³ were performed treating the Ga 3d states as part of the inert core, i.e., not participating in the bonding, while all-electron calculations³⁻⁷ include them in the valence band. The Ga 3d band dispersion was found to be important for total-energy ground state properties because of their overlap with the N 2s band and the relatively short distance (3.18 Å) between Ga atoms in GaN, which is only slightly larger than those in bulk Ga [orthorhombic Ga has bond distances varying between 2.44 and 2.80 Å (Ref. 14)]. The inclusion of the Ga 3d states among the valence states was also found to influence the band gap. These effects were first noted by Lambrecht and Segall⁴ and recently analyzed in detail by Fiorentini *et al.*⁶ and Wright and Nelson.¹² Somewhat different conclusions were obtained regarding the question of whether the inclusion of Ga 3d among the valence states expands or contracts the lattice constant. We discuss the origin of this apparent discrepancy.

The second purpose of this paper is to discuss experimental probes of the Ga 3d states and the valence bands such as x-ray photoelectron spectroscopy (XPS). We present experimental XPS results for zinc blende and

wurtzite GaN. Comparison with the calculated densities of states (DOS) clearly shows that emission from Ga 3d states occurs ~ 3 eV below that of the N 2s bands in conflict with the LDA single particle theory. This discrepancy is explained in terms of self-energy effects as calculated using the so-called Δ SCF or difference of self-consistent-fields approach, in which the binding energy of a localized state is calculated as a total-energy difference. The justification of this approach and the way we implement it will be discussed below.

There has been one previous experimental study of the GaN valence bands by XPS (Ref. 15) and one study using UV-photoemission spectroscopy (UPS).¹⁶ Both of these studies were limited to the wurtzite structure, which is the equilibrium phase. Recently, it proved possible to stabilize the zinc blende polytype of GaN by epitaxial growth on GaAs.¹⁷ Characteristic differences between the spectra in agreement with calculated densities of states are pointed out.

II. EXPERIMENT

The zinc blende samples of GaN were grown on {001} GaAs substrates while the wurtzite layers were grown on {0001} sapphire. The cleaned substrates were mounted on Mo blocks using In solder and transferred quickly into the vacuum. Nitride growth was performed by an electron cyclotron resonance (ECR) plasma enhanced molecular beam epitaxy technique described in detail elsewhere.¹⁷ GaN was grown at 670 °C at a rate of 300 Å/h. The growth on sapphire was initiated with a 300 Å AlN bufferlayer grown at 650 °C after several minutes exposure of the substrate to the nitrogen plasma. The GaAs substrates were outgassed and the oxide desorbed in the conventional manner. A GaAs buffer layer

was grown in order to obtain a clean, defect free initial surface for zinc blende heteroepitaxy. Then, the Ga flux was stopped leaving the substrate under an As overpressure while the nitrogen ECR plasma source was lit. GaN growth was initiated by simultaneously closing the As shutter and opening the Ga and ECR shutters. GaN was heavily doped with Si to avoid charging problems during the XPS measurement. The cubic structure of the film was demonstrated by reflection high energy electron diffraction during growth. The surface was unreconstructed 1×1 with epitaxial relationship GaN(001)||GaAs(001) and GaN[100]||GaAs[100] as expected. The structure was verified after growth by x-ray diffraction.

X-ray photoemission spectroscopy measurements of the valence-band spectra were performed on a Perkin Elmer PHI 5300 ESCA system. The XPS chamber is vacuum connected to the nitride growth system and the transfers between the chambers occurred under ultra-high vacuum conditions (1×10^{-9} Torr). No evidence of surface oxidation was detected by XPS in a sample intentionally left in the transfer tube for several hours. The duration of a typical transfer was five minutes. The XPS spectra were obtained using Al $K\alpha$ radiation ($h\nu = 1486.6$ eV) with a linewidth of ~ 0.6 eV. The escape depth for the photoelectrons is estimated to be ~ 25 Å. Data were collected at an electron emission angle of 45° .

III. COMPUTATIONAL METHOD

The theoretical framework of our study is density functional theory (DFT) (Ref. 18) in the local density approximation (LDA) as parametrized by Hedin and Lundqvist.¹⁹ The band-structure method employed is the linear muffin-tin orbital (LMTO) method in the atomic sphere approximation²⁰ including the combined correction and empty spheres in the usual manner. Equal size spheres were used for Ga and N. A more complete description of the band structures was given elsewhere.^{4,5} Here, we are mainly concerned with the treatment of the Ga 3d orbitals and the DOS. These were calculated using the tetrahedron approximation^{21,22} with a division of the axes of the reciprocal unit cell in 16 divisions and using symmetry reduction to an irreducible set of k points. The treatment of the Ga 3d states forms the main subject of this paper and is discussed along with the results. The Δ SCF approach used to calculate core-hole excitations more accurately will also be described along with the results.

IV. RESULTS

A. Ground state properties

We have performed calculations for GaN in two distinct ways: (1) treating Ga 3d as a core level and (2) as a valence band. Treating the Ga 3d state as a core state in our calculation means imposing atomlike

boundary conditions on its wave function at the Wigner-Seitz sphere radius. The core level and its associated charge density are allowed to relax to self-consistency and thus to adjust to the lattice constant. This treatment is clearly different from a “frozen-core” (or frozen overlapping core⁶) approximation which is more closely related to the pseudopotential treatment as has been discussed in detail by Fiorentini *et al.*⁶ What happens in our Ga 3d corelike treatment is that the core wave functions are artificially compressed in the small Ga spheres and thus have a relatively high kinetic energy. The system can lower its energy by expanding the lattice constant. Hence in our Ga 3d corelike treatment we find a lattice constant of 4.61 Å which is $\sim 2\%$ larger than, and consequently a bulk modulus $\sim 3\%$ smaller than the results from our calculations which includes Ga 3d band dispersion. Our values obtained for the lattice constant and bulk modulus treating Ga 3d as bands are $a = 4.48$ Å and 200 GPa, respectively. These are in excellent agreement with full-potential LMTO calculations.^{6,7} The overestimate of the lattice constant in our Ga 3d core treatment leads to an underestimate of the gap because the hydrostatic band-gap deformation potential is negative. Our calculated value for the latter, $dE_g/d \ln V = -6.6$ eV, implies an underestimate of the gap by about -0.4 eV. In our self-consistent band-structure calculations with Ga 3d treated as core throughout the iterations, the potential is adjusted self-consistently and leads to a final gap which is smaller than the correct gap (obtained with Ga 3d as bands) by only -0.2 eV. The direct hybridization effect of the Ga 3d on the valence-band maximum at a fixed lattice constant is even smaller. This follows from perturbation theory²⁴ since it lies more than a Rydberg away. In fact, if one recalculates the bands keeping the potential determined self-consistently including the effect of Ga 3d fixed but using a basis set that does not include Ga 3d [which can be done by choosing the LMTO linearization energy $\epsilon_\nu(\text{Gad})$ in the conduction band], one finds a gap which is reduced by only 0.1 eV. The latter calculation corresponds to a “two-panel” calculation of the bands.

Our conclusions on the effects of treating Ga 3d as a core state differ from what is obtained in pseudopotential treatments or frozen-core treatments. As explained by Fiorentini *et al.*,⁶ the main additional error made by the pseudopotential method is linearizing core-valence exchange. Even when this is corrected for, the frozen-core approximation leads to a slight underestimate of the lattice constant. In pseudopotential calculations, somewhat arbitrary details on exactly how the pseudopotential is constructed (e.g., the choice of cutoffs in local and nonlocal parts) and the convergence of the basis set can make a difference.

B. X-ray photoemission spectroscopy results and Δ SCF approach

Having convinced ourselves that treating the band character of Ga 3d is important for a correct treatment of the bonding, we now turn to its observation by XPS.

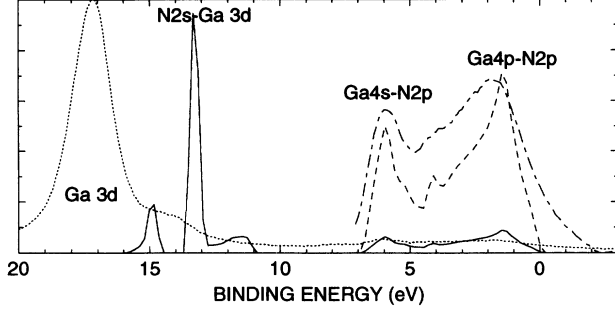


FIG. 1. Measured XPS spectrum and theoretical DOS of wurtzite GaN. The dotted line gives the raw data. The dashed-dotted line differs by a background subtraction and a scale factor chosen so as to magnify the upper valence-band region. The experimental spectrum and theoretical DOS (full line) are aligned by the 6 eV peak. The DOS in this calculation includes Ga 3d–N 2s hybridization effects and is not in agreement with experiment in the region below 10 eV. The dashed curve is a blowup of the DOS in the upper region allowing better comparison to experiment.

An overview of the XPS spectrum of zinc blende GaN in the binding energy range 0 to 20 eV is shown in Fig. 1, with the theoretical DOS superposed. The theoretical and experimental spectra were aligned at the sharp peak at 6 eV binding energy measured from the theoretical valence-band maximum. In this calculation, the Ga 3d is treated as a band state and appears at 13.3 eV. The N 2s states form bonding and antibonding states appearing as peaks on either side of the main Ga 3d peak. The experimental binding energy of the Ga 3d peak, however, is 17.1 ± 0.1 eV below the valence-band maximum. The latter is in good agreement with previous XPS and UPS measurements.^{15,16}

To explain this discrepancy with LDA band theory, we first note that DFT is not directly applicable to one-particle excitations. While for broad valence bands, the LDA Kohn-Sham eigenvalues ϵ_{nk} , which are obtained from

$$\left[-\frac{\hbar^2}{2m}\Delta + v_H(\mathbf{r}) + v_{xc}(\mathbf{r}) \right] \psi_{nk}(\mathbf{r}) = \epsilon_{nk} \psi_{nk}(\mathbf{r}), \quad (1)$$

where v_H is the Hartree potential combining the electron and nuclear electrostatic potential, and v_{xc} is the exchange-correlation potential, are close to quasiparticle excitation energies E_{nk} , given by

$$\begin{aligned} \left[-\frac{\hbar^2}{2m}\Delta + v_H(\mathbf{r}) \right] \Psi_{nk}(\mathbf{r}) \\ + \int \Sigma_{xc}(\mathbf{r}, \mathbf{r}', E_{nk}) \Psi_{nk}(\mathbf{r}') d^3r' = E_{nk} \Psi_{nk}(\mathbf{r}), \end{aligned} \quad (2)$$

with $\Sigma_{xc}(\mathbf{r}, \mathbf{r}', E_{nk})$ the nonlocal and energy dependent exchange-correlation self-energy operator, this is not so for narrow bands, such as the Ga 3d shallow core state.

For the latter, the so-called Δ SCF approach²⁵ provides an alternative to solving Eq. (2). In this approach, one

calculates the binding energy of the core hole $E_B(c)$ as the difference between two self-consistent total energies, one in which the core state is occupied by the electron and one in which the electron is removed. This procedure is intuitively justified within DFT because the presence of a core hole can be viewed as an additional external potential to the valence electrons. The problem is that one now has to treat a localized core hole and thus the problem is equivalent to that of an impurity atom. In fact, the assumption behind this model is that the photoemission process is fast on the scale of the hopping time associated with the bandwidth. In other words, the core hole is assumed to stay localized on the site where it was created during the time of the photoemission process.

The Δ SCF was originally introduced in the context of Hartree-Fock theory and thus derives its name from difference of two self-consistent total energies. In that case, it corrects Koopmans' theorem²³ for the final state or relaxation effects. In the context of DFT, it has an additional effect since Koopmans theorem is not valid in DFT, i.e., $|\epsilon_{nk}|$ do not have the meaning of binding energies.

We first examine how the Δ SCF approach for the core hole binding energy differs from the LDA Kohn-Sham eigenvalue in the free atom. Atomic LDA calculations for Ga yield

$$-\epsilon_{3d}^{\text{atom}} = 19.8 \text{ eV} \quad \text{and} \quad E_B^{\Delta\text{SCF,atom}}(3d) = 28.4 \text{ eV}, \quad (3)$$

which differ by 8.6 eV. One may also calculate the Δ SCF energy by means of Slater's transition state approach^{26,27} as $E_B(c) \approx -\epsilon_c(1/2)$. In the present case, we obtain $-\epsilon_{3d}^{\text{atom}}(1/2) = 28.2$ eV.

The effect of embedding the core-hole excited atom in the solid is that the latter is screened by the valence electrons. Even in semiconductors, the induced screening charge is mostly localized within an atomic Wigner-Seitz sphere.²⁹ The reason for that is that the wave vector dependent dielectric function $\epsilon(q)$ has a characteristic decay the Thomas-Fermi wave vector,²⁹ the inverse of which is comparable to atomic sphere radii. This suggests that as in metals, one can mimic the effect of the induced charge density by means of the so-called *excited-atom approach* of Williams and Lang.²⁸ In this approach, one adds an electron to the first available empty atomic state (here 4p) as the electron is being removed from the core state. Again representing this process by means of the transition state²⁶ approach, the shift between free atom and embedded atom is given by

$$\Delta^{\text{solid}} = -\epsilon_{3d}(3d^{9.5}, 4p^{1.5}) + \epsilon_{3d}(3d^{9.5}, 4p^1), \quad (4)$$

which equals -4.0 eV. Combining the two corrections, we predict the Ga 3d position to be $8.6 - 4.0 = 4.6$ eV below the LDA band position. This slightly overestimates the shift since it would place the Ga 3d at 17.9 eV instead of the experimentally observed value of 17.0 eV.

We note that a reduced screening (i.e., not localized within the Ga sphere) would worsen the agreement. On the other hand delocalizing the hole, in accordance with

the above noted importance of band dispersion for Ga 3d would provide a correction in the right direction. This indicates that the Δ SCF treatment is only approximately valid for this semicore state. A calculation based on Eq. (2) would be interesting, but is beyond the scope of the present paper. We note that even in Cu, the position of the 3d band is 0.5 eV too high in LDA. As the 3d states become narrower, the effect increases. See, e.g., Sec. F, p. 738 in Jones and Gunnarsson²⁵ for further discussion. Notably, the correction is 3 eV for bulk Ga,²⁵ which is only 1 eV smaller than found here. This is consistent with the larger bandwidth in bulk Ga which in turn is related to the closer Ga-Ga distance.

We now turn to a detailed examination of the upper valence band and the N 2s band. The proper band structure to compare with XPS is the quasiparticle spectrum E_{nk} from Eq. (2) rather than the Kohn-Sham band structure ϵ_{nk} obtained from Eq. (1). The excited atom Δ SCF model shows that the Ga 3d excitation lies well below the N 2s band. Instead of actually solving Eq. (2), we can incorporate the changes in quasiparticle band structure from ϵ_{nk} to E_{nk} in a somewhat *ad hoc* manner. In the LMTO method, this can be done in two ways. The first way is to remove the Ga 3d's completely from the spectrum under consideration by changing the linearization energy ϵ_v for the *d*-partial waves of Ga to a value where the latter become 4*d*-like instead of 3*d* like: i.e., ϵ_v is placed sufficiently high (i.e., a few eV) in the conduction band. We then recalculate the bands and DOS with this basis set while keeping the potential fixed. This amounts to a two-panel calculation for the final iteration

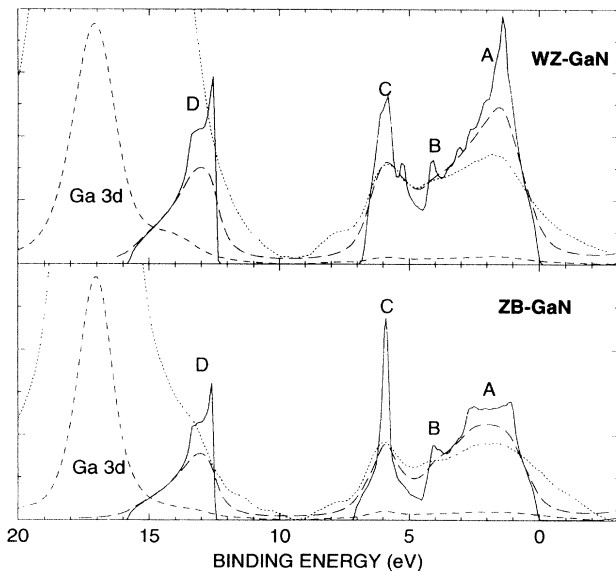


FIG. 2. Measured XPS spectrum and calculated DOS for wurtzite (upper panel) and zinc blende (lower panel) GaN. The DOS in these figures do not include Ga 3d-N 2s hybridization. The solid curve gives the unbroadened DOS, the long-dashed curve includes a Lorentzian broadening of 0.4 eV. The short-dashed line gives the experiment with a scale factor allowing one to see the Ga 3d region, the dotted line is the same spectrum but with the upper part magnified.

as we already mentioned in connection with the total energy and band-gap calculations. The second way is to explicitly include the shift of the Ga 3d “center of the band” potential parameter (C_l in the notation of Ref. 20.) This is similar in spirit to an “LDA+*U*” calculation,³⁰ except for the fact that we here only include *U* as a correction in the final iteration. Both procedures give essentially the same result for the upper bands and for N 2s.

The DOS resulting from the first procedure for both wurtzite (upper panel) and zinc blende (lower panel) are shown by the full lines (unbroadened) and long dashed lines (after Lorentzian broadening by 0.4 eV) in Fig. 2 along with the XPS results (dotted and short-dashed lines corresponding to different scale factors).

We note that the characteristic shape differences of the spectra in the upper valence band are in fair agreement between theory and experiment. Specifically, these are a sharper *A* feature and a slightly reduced intensity ratio of features *C/A* in wurtzite compared to zinc blende. Even the weaker feature *B* is recognizable in the experiments. The peak *C* is mainly related to Ga4*s*-N 2*p* bonding states while peak *A* corresponds to Ga4*p*-N 2*p* bonding states, the dominant character being N 2*p* in both cases. In both cases, we find that when peak *C* is adjusted in intensity to the broadened DOS, peak *A* is more intense in theory than in experiment. This may partially be a result of different matrix elements for states involving the Ga 4*s* and Ga 4*p* components. In fact, the UPS data of Hunt *et al.*¹⁶ indicate that the intensity ratio of peaks *A/C* decreases as one goes to higher photon energies. This is an indication that matrix elements are indeed responsible.

Feature *D* which corresponds to the N 2s band appears as a shoulder on the broad and intense Ga 3d emission in the experiment. The peak positions in the upper valence

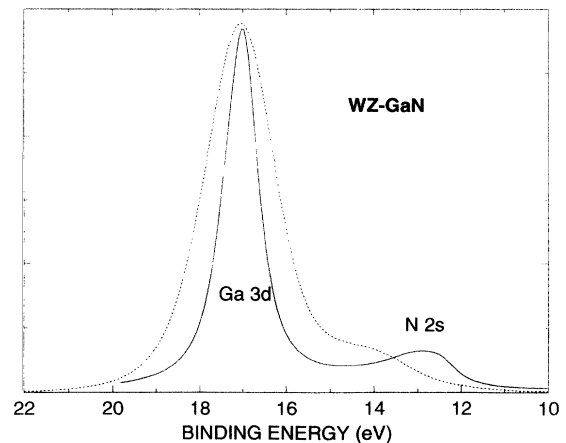


FIG. 3. Measured XPS spectrum (dotted line) and calculated DOS (full line) of wurtzite GaN in the Ga 3d-N 2s range. An additional background subtraction was made in this energy range so as to make the spectrum go to zero at 22 eV. The DOS in this figure was obtained by adding a semiempirical shift of 4 eV to the Ga 3d band center and includes a Lorentzian broadening of 0.4 eV. The upper bands (not shown) were positioned as in Figs. 1 and 2. A ~ 1.2 eV discrepancy between the theoretical N 2s and experimental shoulder positions is apparent.

band agree well between theory and experiment indicating that the many-body effects responsible for the Ga 3d band shift are small for N 2p. The theoretical N 2s band position, however, is about 1.2 ± 0.2 eV above the shoulder position indicating that a self-energy shift is also required for the fairly narrow N 2s band. This can be seen more clearly in Fig. 3. In this figure the DOS was calculated including a shifted Ga 3d band (second procedure). By including broadening, we see the N 2s appearing as a shoulder on the Ga 3d peak although they are actually well separated bands. The origin of the 1.2 ± 0.2 eV shift is essentially the same as for the Ga 3d peak, namely, the differences between E_{nk} and ϵ_{nk} . Unfortunately, the excited atom model Δ SCF approach, however, is not applicable to the N 2s state because it cannot adequately be described as a semicore level. In other words, the width of this band invalidates the assumption that the core hole stays localized as assumed in the Δ SCF model. We thus cannot easily make an estimate of this shift.

V. CONCLUSIONS

In conclusion, the semicore nature of the Ga 3d states leads to important effects on the bonding in GaN. The close distance between Ga atoms and the near resonance in energy of the Ga 3d and N 2s LDA eigenvalues leads to considerable band dispersion and overlap with the N 2s band. Its effects on the band gap are mostly indirect through the resulting effects on the lattice constant. The quasiparticle excitation energy of the Ga 3d as probed by

XPS, however, is about 4 eV deeper below the valence-band edge than predicted by LDA eigenvalues and clearly below the N 2s band. This indicates that, in spite of the band character, the self-energy effects on this narrow band are substantial. The Δ SCF approach combined with the excited-atom model yields a value of 4.6 eV for the shift. The overestimate of the shift by the Δ SCF method is consistent with the *semicore* nature of these states. The upper valence band features are in good agreement with XPS including the differences between zinc blende and wurtzite, while the experiment indicates that the LDA result for the N 2s state needs a downward self-energy correction of ~ 1.2 eV. Finally, we note that similar effects to the ones described here for Ga 3d in GaN are expected for In 4d in InN.

Note added in proof. After completion of this work, we noted that the quasiparticle band-structure calculations of GaN by Rubio *et al.*³¹ obtain a ~ 2 eV downward shift of the N 2s band, in good agreement with the present work.

ACKNOWLEDGMENTS

The work at CWRU was supported by NSF Grant No. DMR92-22387. The work at UIUC was supported by ONR Grant No. N00014-89-J-1780. A. Agarwal and A. Rockett acknowledge support by DOE under Contract No. DEFG02-91-ER-45439. S. Strite was supported financially by the AFOSR. We also gratefully acknowledge technical assistance of D. Jeffers.

* Present address: IBM Zürich Research Division, Rüschlikon, Switzerland.

¹ For a comprehensive review of recent developments in nitride research, see S. Strite and H. Morkoç, *J. Vac. Sci. Technol. B* **10**, 1237 (1992).

² I. Akasaki and H. Amano, in *Wide Band Gap Semiconductors*, edited by T. D. Moustakas, J. I. Pankove, and Y. Hamakawa, MRS Symposia Proceedings No. 242 (Materials Research Society, Pittsburgh, PA, 1992), p. 383, and references therein.

³ I. Gorczyca and N. E. Christensen, *Solid State Commun.* **80**, 335 (1991).

⁴ W. R. L. Lambrecht and B. Segall, in *Wide Band Gap Semiconductors* (Ref. 2), p. 367.

⁵ W. R. L. Lambrecht and B. Segall, in *Properties of the Group-III Nitrides*, edited by J. H. Edgar, EMIS Data Review Series (IEE, Stevenage, Herts, United Kingdom, 1994).

⁶ V. Fiorentini, M. Methfessel, and M. Scheffler, *Phys. Rev. B* **47**, 13353 (1993).

⁷ K. Kim, W. R. L. Lambrecht, and B. Segall, *Phys. Rev. B* **50**, 1502 (1994).

⁸ A. Muñoz and K. Kunc, *Phys. Rev. B* **44**, 10372 (1991).

⁹ P. E. Van Camp, V. E. Van Doren, and J. T. Devreese, *Solid State Commun.* **81**, 23 (1992).

¹⁰ M. Palummo, C. M. Bertoni, L. Reining, and F. Finochi, *Physica B* **185**, 404 (1993).

¹¹ B. J. Min, C. T. Chan, and K. M. Ho, *Phys. Rev. B* **45**, 1159 (1992).

¹² A. F. Wright and J. S. Nelson, *Phys. Rev. B* **50**, 2159 (1994).

¹³ J. Neugebauer and C. G. Van de Walle, in *Diamond, SiC and Nitride Wide-Bandgap Semiconductors*, edited by C. H. Carter, Jr., G. Gildenblat, S. Nakamura, and R. J. Nemanich, MRS Symposia Proceedings No. 339 (Materials Research Society, Pittsburgh, 1994).

¹⁴ R. W. G. Wyckoff, *Crystal Structures*, 2nd ed. (Interscience, New York, 1963), Vol. 1, p. 23.

¹⁵ J. Hedman and N. Mårtensson, *Phys. Scr.* **22**, 176 (1988).

¹⁶ R. W. Hunt, L. Vanzetti, T. Castro, K. M. Chen, L. Sorba, P. I. Cohen, W. Gladfelter, J. Van Hove, A. Kahn, and A. Franciosi, *Physica B* **185**, 415 (1993).

¹⁷ S. Strite, J. Ruan, Z. Li, A. Salvador, H. Chen, D. J. Smith, W. J. Choyke, and H. Morkoç, *J. Vac. Sci. Technol. B* **9**, 192 (1991).

¹⁸ P. Hohenberg and W. Kohn, *Phys. Rev.* **136**, B864 (1964); W. Kohn and L. J. Sham, *ibid.* **140**, A1133 (1965).

¹⁹ L. Hedin and B. I. Lundqvist, *J. Phys. C* **4**, 2064 (1971).

²⁰ O. K. Andersen, O. Jepsen, and M. Šob, in *Electronic Band Structure and Its Applications*, edited by M. Yussouff

- (Springer, Heidelberg, 1987), p. 1.
- ²¹ O. Jepsen and O. K. Andersen, *Solid State Commun.* **9**, 1763 (1971).
- ²² P. E. Blöchl, O. Jepsen, and O. K. Andersen (unpublished).
- ²³ T. Koopmans, *Physica (Utrecht)* **1**, 104 (1934).
- ²⁴ W. R. L. Lambrecht, B. Segall, and O. K. Andersen, *Phys. Rev. B* **41**, 2813 (1990).
- ²⁵ R. O. Jones and O. Gunnarsson, *Rev. Mod. Phys.* **61**, 689 (1989).
- ²⁶ J. C. Slater, *The Self-Consistent Field for Molecules and Solids* (McGraw-Hill, New York, 1974), Vol. 4, p. 35.
- ²⁷ W. R. L. Lambrecht, *Phys. Rev. B* **34**, 7421 (1986).
- ²⁸ A. R. Williams and N. D. Lang, *Phys. Rev. Lett.* **40**, 954 (1978).
- ²⁹ N. J. Castellani and W. R. L. Lambrecht, *Phys. Status Solidi B* **151**, 565 (1989); W. Lambrecht, N. J. Castellani, and D. B. Leroy, *Solid State Commun.* **56**, 1073 (1985).
- ³⁰ V. I. Anisimov, I. V. Solvyev, M. A. Korotin, M. T. Czyżyk, and G. A. Sawatzky, *Phys. Rev. B* **48**, 16 929 (1993).
- ³¹ A. Rubio, J. L. Corkill, M. L. Cohen, E. L. Shirley, and S. G. Louie, *Phys. Rev. B* **48**, 11 810 (1993).